POLITECNICO DI TORINO
Repository ISTITUZIONALE

Stability of foam-aggregate mixtures for EPB tunnelling

Original
Stability of foam-aggregate mixtures for EPB tunnelling / Carigi, A., Todaro, C.. - In: TUNNELLING AND UNDERGROUND SPACE TECHNOLOGY. - ISSN 0886-7798. - 173:(2026). [10.1016/j.tust.2026.107621]

Availability:
This version is available at: 11583/3014631 since: 2026-08-19T08:31:04Z

Publisher:
Elsevier

Published
DOI:10.1016/j.tust.2026.107621

Terms of use:

This article is made available under terms and conditions as specified in the corresponding bibliographic description in the repository

Publisher copyright

(Article begins on next page)

13 October 2026

Tunnelling and Underground Space Technology 173 (2026) 107621

Contents lists available at ScienceDirect

Tunnelling and Underground Space Technology incorporating Trenchless Technology Research

journal homepage: www.elsevier.com/locate/tust

Stability of foam-aggregate mixtures for EPB tunnelling

Andrea Carigi [a,*], Carmine Todaro [a]

[a] Politecnico di Torino, Corso Duca degli Abruzzi 24, Torino 10129, Italy

ARTICLE INFO

Keywords:
EPB tunnelling
Soil conditioning
Foam stability
Half-life time
Grain size distribution

ABSTRACT

In Earth Pressure Balance (EPB) tunnelling, soil conditioning through foam injection is critical for successful excavation. However, a significant knowledge gap exists between methodologies used to assess foam stability and those employed to evaluate conditioned soil stability. This study addresses this gap by investigating the stability of foam-aggregate mixtures under controlled laboratory conditions, progressively adding solid particles of a reference soil to foam and evaluating temporal stability changes. The experimental investigation examined various particle concentrations and size distributions to understand their influence on foam stability mechanisms. Results confirm that particle inclusion significantly enhances foam stability, with stability increasing exponentially with solid fraction (m_x) and decreasing according to a power law with particle diameter. These effects become significant for solid fractions exceeding 50 g per 125 g of liquid generator and for particles smaller than 0.25 mm in diameter. The study demonstrates that contributions from different granulometric fractions compound linearly, and foam-solid mixture stability can be expressed as an exponential function of total particle surface area. This relationship explains why finer particles exhibit greater stabilizing effects. While some behavioral aspects were partially anticipated in literature, previous research did not fully account for larger particle diameter effects. Despite promising findings, the study could not completely bridge the gap between foam stability and conditioned soil stability, as the minimum achievable Foam Injection Ratio (FIR) remains an order of magnitude higher than typically used for soil conditioning. Nevertheless, this research successfully narrows the existing knowledge gap and provides valuable insights into solid fraction roles in foam stabilization. The findings enhance understanding of foam-soil mixture behavior, contributing to improved soil conditioning strategies and more effective EPB tunnelling operations. This work establishes a foundation for future research aimed at completely connecting foam stability and conditioned soil stability assessment methodologies.

1. Introduction

In EPB tunnelling, a key aspect for the correct management of the excavation is soil conditioning, which consists in the mixing of foam and other conditioning agents with soil to temporally modify its behaviour and make it suitable to be excavated with this technology (Vinai et al., 2008; Budach and Thewes, 2015; Mori et al., 2018). Being the newly acquired properties temporary due to the instability of foam, to achieve a holistic design approach, it is important to evaluate also the time-stability of conditioned soil to optimise the interplay between the excavation phase, the excavated soil management on the jobsite and its reuse after the used foam and conditioning agents have been bio-degraded (Firouzei et al., 2020; Peila et al., 2022; Oñate and Murt, 2022).

An important factor for the successful use of EPB technology is the stability of the foam used in the soil conditioning process, which must remain stable for a sufficient period to: ensure homogeneous mixing with the soil, allow for adequate pressure transmission at the face, and preserve the conditioned soil's workability throughout the excavation. To evaluate these aspects, despite being important the stability of the foam itself, it is more important to assess the stability of foam mixed with soil.

From these considerations arises the necessity to further study the time-stability of conditioned soil. Concerning this research field, some authors focused on the stability of the conditioned soil as a whole, often limitedly on particular soils with fixed grain size distribution (Peila et al., 2008; Riviera et al., 2014; Oggeri et al., 2014; Pedraza Peña et al., 2015; Djeran-Maigre et al., 2018; Wu et al., 2018; Zumsteg et al., 2018; Carigi et al., 2020; Luo et al., 2022; Carigi et al., 2023; Wu et al., 2024), while several other researchers focused on the stability of the foam by itself. Some of these latter researches belong to the field of EPB tunnelling, while many other researches are developed in scientific

* Corresponding author.
E-mail address: andrea.carigi@polito.it (A. Carigi).

https://doi.org/10.1016/j.tust.2026.107621
Received 22 July 2025; Received in revised form 1 January 2026; Accepted 9 March 2026
Available online 17 March 2026
0886-7798/© 2026 The Authors. Published by Elsevier Ltd. This is an open access article under the CC BY-NC-ND license (http://creativecommons.org/licenses/by-nc-nd/4.0/).

fields different from tunnelling (EFNARC, 2005; Wierenga et al., 2009; Zhang et al., 2015; Jones et al., 2016; Li et al., 2022; Grossmann et al., 2020; Moll et al., 2020; Zhao et al., 2021; Carigi et al., 2023; Chen et al., 2024).

Between these two classes of researches a scientific gap is present since, despite several authors investigated the behaviour of foam-solid particles mixes, it never concerned the research field related to tunnelling and soil conditioning. More in detail, Li et al. (2022) produced foams both with a thixotropic polymer and silica nanoparticles (7–40 nm) and then performed an analysis of their stabilities. They found that as the concentration of the aforementioned particles increases there is an increment of foam stability. Instead, the foamability, the volume produced with fixed conditions, reaches a maximum for a specific concentration of particles and then decreases. Hunter et al. (2009) studied the interaction between surfactants and silica nanoparticles highlighting that the interaction between surfactants and particles to stabilise foams. Horozov (2008) performed an extensive research on super-stabilized foams through the addition of silica nanoparticles and found that the stability of foams is strongly dependent on shape, size, concentration and hydrophobicity of the solid particles. Moreover, AlYousef et al. (2018) performed stability tests on foams produced with surfactants and silica nanoparticles finding a significant stability increment. Concerning the methods used by these researchers, Hunter et al. (2009), Horozov (2008)) and AlYousef et al. (2018) produced the foam by manually shaking a glass tube with the foaming solution inside. This method produces foams significantly different from the ones used in tunnelling, since the method used by these authors enables the production of foams with FER, Foam Expansion Ratios (i.e. the ratio between the volume of foam and the volume of the liquid used to produce it), much lower than the one used in tunnelling, leading to an impossibility to directly transfer the knowledge aquired with these researches to the field of tunnelling without further tests and validation of the results.

Fameau and Salonen (2014) discussed the role of particles of different type and origin on the stability of foams. They found that hydrophobic particles mainly de-stabilize foams while hydrophilic particles have a stabilizing effect. The authors focused on the effect of nanometric particles and did not analyse the effect of micrometric or millimetric ones. These results cannot be directly applied to the case of EPB conditioning since a relevant part of the particles constituting soil have equivalent diameter in the range of millimetres and micrometres.

Zhang et al. (2015) studied the stability of foams in which particles of starch were added and found that it affected both stability and foamability. In particular, as the viscosity increases due to the starch addition the stability increases as consequence of the reduction of drainage in foams. Moreover, the foamability reduces as the starch concentration increases because the higher viscosity reduces the amount of incorporated air for a standard mixing energy. Also, the starch molecules adsorb some of the surfactant reducing the effective concentration and, consequently, the foamability. These results, being obtained for starch particles, need to be validated for soil particles.

Peña Duarte (2007) tried to approach the problem by using actual soil, measuring the half-life time of both foams and conditioned sands. By using sands coarser than 1 mm, the author found that for this very specific case the foam stability was not significatively influenced, a result that cannot be generalised to conditioned soils due to the absence of all the soil fractions smaller than 1 mm. A similar research was developed by Wu et al. (2020) that performed stability tests on foams-sand mix by using a soil with a grain size distribution roughly spanning between 5 mm and 0.1 mm. In this case the author, despite assessing the shortcoming of the previous author, analysed the stability through the dimensional distribution of bubbles in time using a microscope while drainage measurements were not involved in the tests.

Recently, Schröer et al. (2023) achieved the production of a foam with solid particles for EPB applications using a specifically designed foam generator, starting from a high-density bentonite slurry. This foam was used to expand the applicability field of EPB tunnelling but no specific investigation about foam stability was carried out and the dimensions of used particles is consistently smaller than 75 μm.

In summary, these experimental studies, provide valuable insights into the mechanisms governing foam-particles mixtures stability but are often conducted outside the specific context of EPB tunnelling. They show that the presence of solid particles can significantly influence foam performance, depending on particle size, concentration, shape, and surface properties, as well as the rheology of the foaming solution. However, differences in foam production methods and test conditions pose a strong limit to the direct applicability of these findings to the tunnelling field. Hence, further research is needed to assess foam stability under conditions comparable to those encountered during EPB tunnelling.

To fill the gap, in this research the authors tried to understand the change in stability of a mix of foam and actual soil particles ranging from micrometres to millimetres. To achieve this result, for each grain size these particles were added in various quantities to understand how each of these types of particles influences the stability of foam. In the end, different types of particles were added together to simulate the presence of a soil. Differently from what happens in EPB-TBM, the soil was added during the production of foam since to mix sub-millimetric particles with foam, it is needed too much mixing energy and time to obtain a homogenous material, that would in turn dramatically change the properties of the foam itself and confounding the contribution of the presence of soil particles with the one of the energetic mixing. By generating foam with soil particles already in it, the authors aim to understand the contribution of different particles classes to the overall stability of conditioned soil. Due to the extension of the tests conducted, investigations on the role of shape of grains and their hydrophily were not considered in this study but could be part of future development.

2. Materials

2.1. Foam

The foam used in the experimental campaign was produced from a foaming solution consisting of water and a commercial surfactant agent at a volumetric concentration $c_f = 1.0\%$ (v/v). According to the safety data sheet, the surfactant product is composed of:

- 5-chloro-2-methyl-2H-isothiazol-3-one and 2-methyl-2H-isothiazol-3-one (cc $>$ 0.0002% − $<$0.0015%) CAS 55965–84-9;
- Alcohols, C12-14, ethoxulated, sulfates, sodium salts (cc $>$ 10% − $<$20%) CAS: 68891–38-3.

2.2. Aggregates

For the production of different grain size fractions, to be mixed with the foam, the reference soil shown in Fig. 1 was dried out in oven at 110 °C accordingly to UNI EN 933-1 and divided through sieving at 20, 10, 5, 2, 1, 0.5, 0.25, 0.125 and 0.075 mm.

In the following, each fraction will be referred as f_x, where x is the size of the upper sieve's mesh through which the soil passed by (e.g. $f_{0.25}$ is the fraction passing at 0.25 mm and retained at 0.125 mm).

On the passing at 0.425 mm the Atterberg's limits (UNI EN ISO, 2018) have been performed and the material resulted non-plastic since was not possible to roll a tread at any water content as specified by the norm.

3. Methods

3.1. Half-life test modified procedure

To reach a more detailed characterization of the foam decay process, the half-life time test (EFNARC, 2005) has been modified as described in Carigi et al. (2022) and the resulting data were analysed.

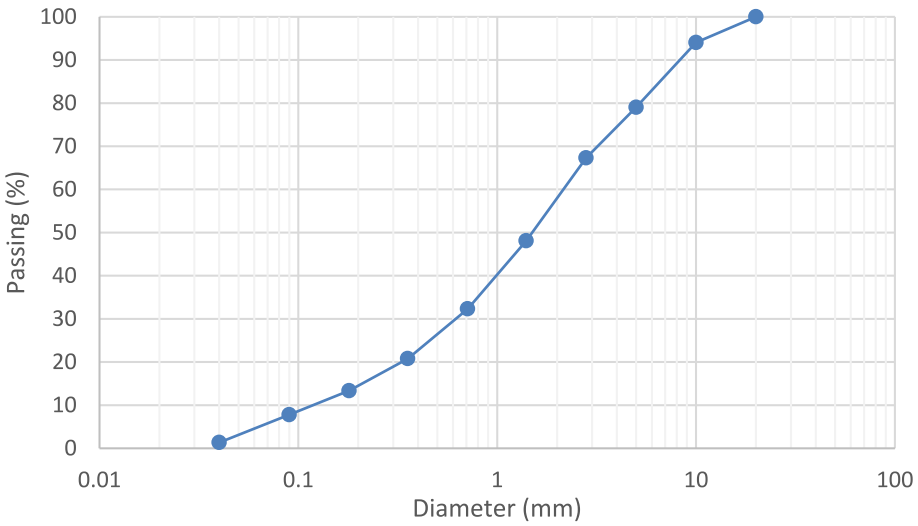

Fig. 1. Grain size distribution of the reference soil.

To describe the whole degradation process of the foam, a continuous sampling of the weight of the drained foaming solution was applied. The used device (Fig. 2) has 3 funnels, each one equipped with a porous stone with high permeability that do not affect the drainage speed, and below each funnel, a bucket to collect the drained liquid was placed. Each funnel and each bucket is equipped with a 0.1 g-precision load cell (LC) and all of them are connected to an Arduino Mega 2560® processor to acquire data with a frequency of 10 Hz. Also, a micro-SD data logger and an LCD screen were installed. In Fig. 3 a scheme of the device is given.

The data log starts as 80 g of foam are inside the funnel and stops when the weight of drained liquid reaches 65 g, (i.e. 80% of the total mass). A stop at higher thresholds was found not useful since, for high amount of drained liquid, the foam drifts away from relevant conditions for tunnelling applications and would greatly increase the required time to carry out the tests and the analysis.

To ensure that there was no delay between the start of degradation of foam and the start of drainage, the porous stones were preventively saturated before each test. To prevent their clogging, due to the presence of solid particles included in the foam samples, a non-woven fabric (NWF) disk was interposed between the foam and the porous stone (Fig. 4).

Furthermore, this method represents an improvement with respect to the current standards (EFNARC, 2005) but differently from the on-site conditions, it conduces the test at atmospheric pressure.

3.2. Foam production

3.2.1. Method A

The generator used for the foam production was already used for numerous researches already carried out at Politecnico di Torino (Vinai et al., 2008; Peila et al., 2007; Peila et al., 2013; Carigi et al., 2022. In Fig. 5 a picture and a scheme of the foam generator are shown. The generator operates with a maximum liquid flow of 11.9 l/min and max air pressure of 4 bar. Given that the stability of foam depends on the flow rate (Bahrami et al., 2024), it was set at 5.6 L/min and kept constant while, to regulate the FER, the air flow rate was changed through needle valves.

The foam generator is equipped with a foam gun (internal diameter 78 mm, length 450 mm, filled with glass fragments of mean diameter of 5 mm). This foam gun is very similar to the type commonly used in EPB-TBMs (Fig. 5).

After the production of foam, for foam and sand or gravel mixtures, the mixing phase can follow the foaming phase, both adding foam to soil or soil to foam, but this approach cannot be used for fine particles. In fact, fine soil forms lumps that are not distributed homogeneously in the foam (Fig. 6) or should be mixed with very high energy and for long time, changing the structure of the used foam. Hence, for the production of the foam, another procedure has to be followed (Method B).

3.2.2. Method B

To produce foam with dispersed particles the stirrer shown in Fig. 7, equipped with the impeller shown in Fig. 8, is used.

The following procedure was used for foam production for all the samples:

1. Production of 125 g of foaming solution with 1% concentration of Product A (123.5 g of water gently mixed with 1.25 g of Product A);
2. Pre-foaming phase for 5 s. The helix reaches 1100 rpm with static mixing (Fig. 9a);

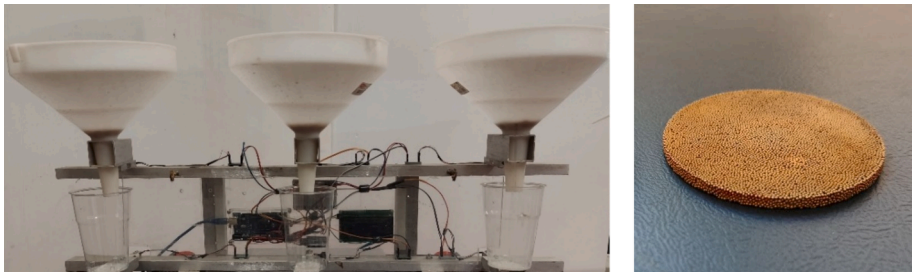

Fig. 2. Left: Modified half-life time device; Right: Porous stone.

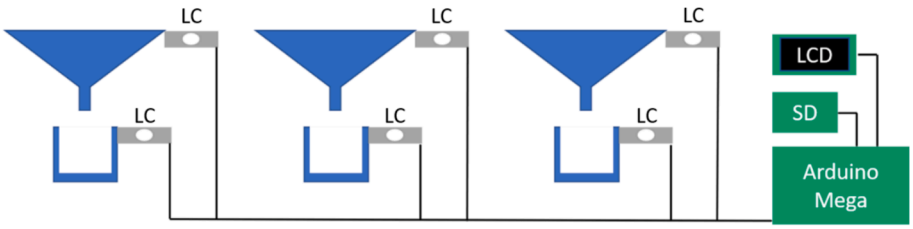

Fig. 3. Scheme of the modified half-life time apparatus.

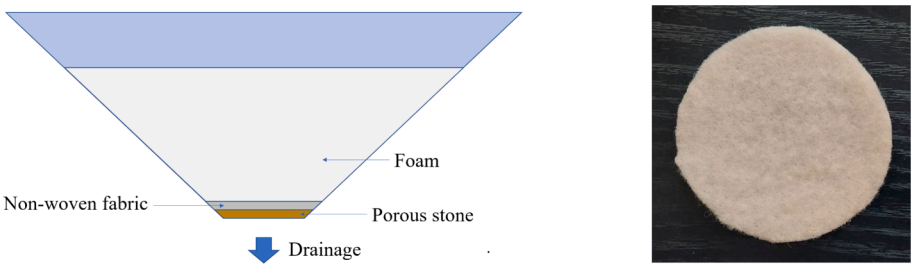

Fig. 4. Left: Position of NWF in the half-life time funnel; Right: Non-woven fabric disk.

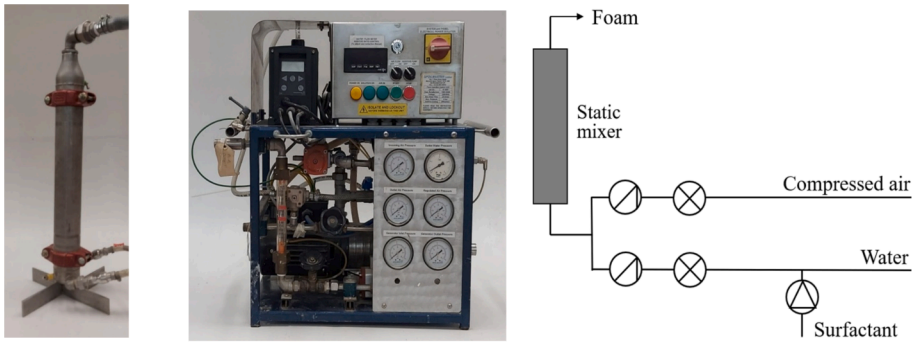

Fig. 5. Foam generator. Left: foam gun; Centre: foam generator; Right: foam generator scheme.

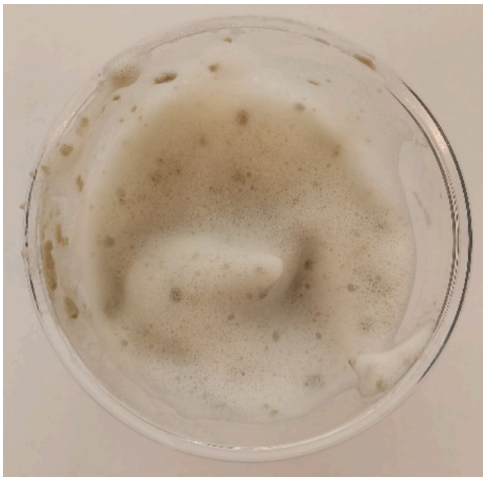

Fig. 6. Foam with clay lumps.

3. Progressive solid particles addition for 40 s. If no solid is added, to create a reference foam without particles, the mixing at 1100 rpm for 40 s was carried out anyway;
4. Acceleration of mixing for 5 s. The helix reaches 2200 rpm;
5. Mixing at 2200 rpm for 10 s;
6. Oscillatory mixing phase (Fig. 9b) for 90 s ± 10 s at 2200 rpm with frequency of vertical oscillations of 0.5 Hz;
7. Start of the half-life test.

For each solid fraction f_x described in Chapter 2.2 a set of samples of foam are produced. To produce each sample, 125 g of foaming solution, was mixed with the following quantities m_x: 0.1 g, 0.5 g, 1 g, 5 g, 10 g, 20 g, 50 g, 100 g. In particular, 100 g was set as a limit due to the physical limitation in the production of homogeneous foam with greater quantities. To produce 80 g of foam to put to test, it was chosen to use 125 g of foaming solution to grant sufficient foam production to ease the transfer from the mixing bucket and the half-life time funnel in a short time to avoid the start of the decay process during the transfer.

Then, an additional set of samples was produced by using 100 g of a mixed solid fraction obtained by with combinations of different proportions of $f_{0.125}$ and $f_{0.075}$ (100–0%, 80–20%, 60–40%, 40–60%, 20–80%, 0–100%) to test the effect of the compresence of different solid fractions on the half-life time.

3.2.3. *Validation of the mixing approach*

To verify the equivalence between the two foaming methods (Method A and Method B), a set of calibration tests was carried out on foams without solid particles produced using the two methods. Also, this phase included both tests carried out with and without the NWF to assess its presence influence.

As first step, the half-life time trend as function of FER was

Fig. 7. Used high speed stirrer.

determined on samples produced with Method A. Then a second set of tests on foam samples produced with Method B were performed. Given the narrower range of FER achievable with Method B compared to Method A, a target FER equal to 15 was aimed during the samples production and an actual average FER of 14.37 was reached. For both types of foam, were carried out tests both with and without NWF.

Fig. 10 shows that, around the target FER, the generation method has no sensible influence on the half-life time. Also, the presence of NWF seems to slightly reduced the half-life time coherently for the two foam-production methods, hence all the tests were performed using the NWF in the setup to prevent the clogging of the porous stones.

Moreover, to verify the homogeneity of the solid fraction across the produced volume of foam, a sample was produced and, then, the obtained foam was divided in 4 subsamples. By drying and weighting the samples, the solid fractions were compared obtaining the results are shown in Table 1.

Between the 4 samples, the maximum difference was of 0.2% in the solid percentage. Hence, the production method gives good homogeneity to the sample.

Given the results shown in Fig. 10 and Table 1 the Method B was considered suitable to the scope of this research.

3.2.4. *Drained mass normalization*

As different solid fraction increases, the composition of the foam is obviously modified leading, for 80 g-samples of foam-aggregate mixture, to have a minor liquid fraction. Hence, the half-life time should not refer to 40 g anymore.

Another issue to face to define a threshold at which set the half-life time has to be considered that not all of the total amount of the foaming solution used to produce the foam is available for drainage. In fact, a part of the liquid fraction is adsorbed on the surface of solid particles. Some tests were conducted to estimate the amount of liquid fraction adsorbed by the solid fraction at very long times and using the maximum solid fraction tested ($m_x = 100$ g). It was found that the mass of adsorbed liquid is at least one order of magnitude smaller than the total amount of water present in the 80 g sample. In Fig. 11 is reported a scheme of the outcomes of a long-time test. Given the relatively small quantity of adsorbed liquid, for simplicity the half-life time was considered the time required to drain half of the liquid mass of the sample of 80 g of foam-aggregate mix (Fig. 11). It should be noted that this is true for this specific kind of soil particles and may be not true for more active kinds of soils.

3.2.5. *FER comparison across different datasets*

When the solid fractions dimension and mass added to the foaming solution change, the FER obtainable with Method B, for constant mixing time, changes too. This phenomenon was already described by some of the cited authors.

To consider the variability of FER obtained with the same procedure applied to foaming solutions for different type and quantity of particles, the ± 10 s variability at point 6 of the Method B was introduced to produce a set of different FERs, and then to proceed with the evaluation of half-life time through linear interpolation at a target FER. This FER was chosen by averaging of the ones obtained for all test sets, with the

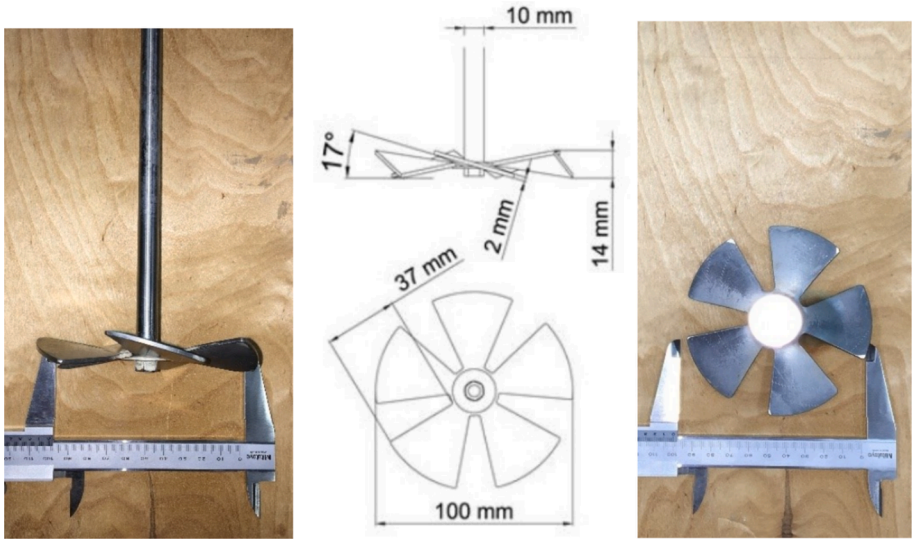

Fig. 8. Impeller used for the production of foam (modified from Todaro et al. 2019).

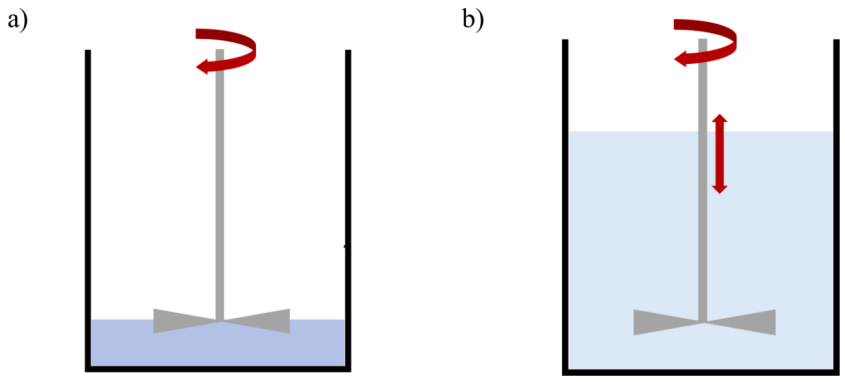

Fig. 9. Mixing methods: a) Static mixing used for Phases 2 to 5, b) Oscillatory mixing used in Phase 6.

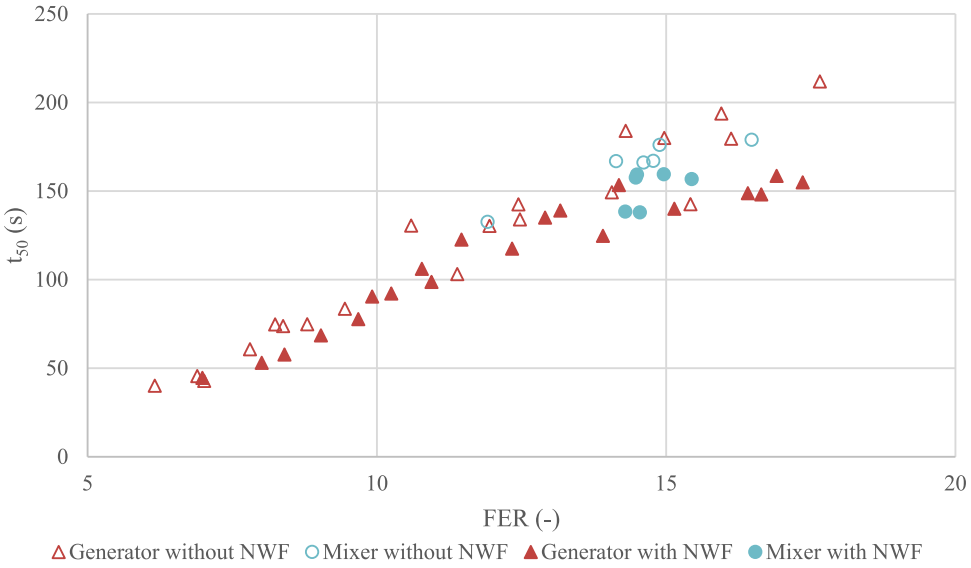

Fig. 10. Comparison between half-life time of samples produced with different generation methods and different test apparatus configurations.

Table 1
Homogeneity of a sample generated with the procedure.

Sample ID	Foam weight (g)	Solid weight (g)	Solid percentage (%)
1	48.69	21.17	43.5
2	49.92	21.65	43.4
3	46.93	20.48	43.6
4	36.64	15.91	43.4

exclusion of the series obtained with 100 g of $f_{0.075}$ and $f_{0.125}$. These two series were excluded because they were strongly diverging from the FER range of all other series, as shown in the following.

For these set of data obtained with 100 g of $f_{0.075}$, instead of an interpolation, the data were linearly extrapolated from the available data despite the inherently higher uncertainties. No other options were given since there was no range of superposition of FERs with the other series.

3.2.6. *Viscosity*

To verify if the hypothesis of Zhang et al. (2015) applies to this context, i.e. that the presence of solid particles increases the viscosity of the foaming solution, some viscosity tests have been carried out on for different mass of solid particles. In this work, with the term "viscosity" the authors refer to the dynamic viscosity. However, hereinafter the only

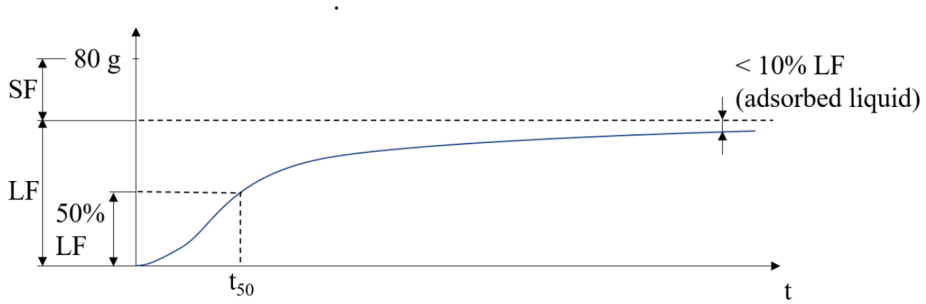

Fig. 11. Relationship between solid fraction (SF) and liquid fraction (LF) for the definition of half-life time of foam-aggregate mixtures.

word "viscosity" has been used for streamline the reading.

The viscosity of 1.0%-solutions of Product A, additioned with solid particles ($f_{0.500}$, $f_{0.250}$, $f_{0.125}$ and $f_{0.075}$) was measured using a rotational viscometer Fungilab shown in Fig. 15.

The viscosity was measured using an LCP spindle for low viscosities (Fig. 12) at 100 rpm and a temperature of 22 ± 2 °C.

4. Results

4.1. Viscosity

On foaming solutions with particles $f_{0.500}$, $f_{0.250}$ and $f_{0.125}$ the viscosity test gave no suitable results because the sedimentation occurred in a time span shorter than the one needed to carry out viscosity tests. The viscosity test on the solution made with $f_{0.075}$, was carried out successfully. A quadratic relationship between the solid fraction mass m_x and viscosity was found in the range 0–100 g of solid mass added to 125 g of foaming solution (Fig. 13), proving the dependence of viscosity on m_x. Hence, according to the hypothesis of Zhang et al. (2015), with m_x increasing should be expected a reduction of FER obtained with the same foaming method and conditions.

4.2. Foamability of single fraction foams

Using the procedure described in chapter 3.2.2 (Method B) to produce foam, the tests shown that the FER of the resulting foam depends on the solid fraction following a quadratic law. Using the fraction $f_{0.075}$, an increment of FER was measured up to $m_x = 20$ g and, then, a decrement of FER for higher quantities of solid fraction. This behaviour shows an analogy to the results, described by Li et al. (2022), on foams produced using nanometric particles. The following tests on foams produced with higher diameter fractions shown a change of the behaviour: the concavity of the curve progressively reduced and then reversed its sign for the fraction $f_{0.500}$ (Fig. 14). The trend of the single coefficients of the quadratic law obtained for different mass fractions are shown in Fig. 15, Fig. 16 and Fig. 17 as function of the solid particle diameter showing a linear correlation between the coefficient of the quadratic law and the solid fraction. In Fig. 14 is also plotted as reference the FER 14.43 obtained using the Method B in absence of solid particles as described in Chapter 3.2.3.

4.3. Half-life time of single fraction foams

To evaluate the half-life time at a target FER of samples of foam produced with soil particles, due to the different foamability of the mixes, Method B was used to achieve a variety of FER. Then, the test results was analysed at the average FER, which is 12.46. In the evaluation of the average FER the samples prepared with 100 g of $f_{0.075}$ and $f_{0.125}$ where excluded due to the observed strong reduction of the foamability. For each series of data, the half-life time was linearly interpolated (Fig. 18 and Fig. 19), with the only exception of 100 g of $f_{0.125}$ and $f_{0.075}$ that were it was linearly extrapolated (Fig. 20 and Fig. 21).

As shown in Fig. 22 the half-life time values decrease when particles with bigger fraction diameter f_x are used and increases when the solid fraction m_x is raised. More in detail, an exponential relationship between the solid fraction and the half-life time was found. Moreover, the exponents of the aforementioned relationships vary with a power law with the diameter of the particle fraction, as shown in Fig. 23. Increasing the diameter of the particles, the exponent tends to 0 and the exponential trend asymptotically tends to the value of foam half-life time without particles (Fig. 22). This result generalises the findings of Peña Duarte (2007) that found no influence on half-life time of foams added with millimetric diameter.

Similarly, a trend showing a power law relationship between the half-life and the particle diameter of the solid fraction (f_x) for all the considered values of solid masses (m_x) (Fig. 24). Again, for m_x that tends to 0, the half-life time tends to the one of foam without particles. Also, for fixed solid fraction m_x, as the diameter of solid fraction f_x increases, the half-life time tends asymptotically to the one of foam without particles. Although the underlying physical mechanisms driving this behaviour remain unclear, the half-life exhibits an exponential dependence on m_x and a power law dependence on f_x.

4.4. Foamability of foams produced with multiple solid fractions

As highlighted in Section 3.3.2, foamability is influenced by both the particle size f_x and the solid fraction m_x. This chapter presents the results of foam production experiments using mixtures with varying proportions of $f_{0.125}$ and $f_{0.075}$.

Considering the very small impact of the biggest used fractions on foamability, $f_{0.500}$ and $f_{0.250}$ were excluded from this section of the study. As shown in Fig. 25, a linear relationship emerges between the percentage of the solid fraction $f_{0.075}$ and the total solid fraction m_x. Notably, the R^2 value exceeds 0.9 when calculated using the average values for each percentage of $f_{0.075}$. This indicates a strong consistency in the linear trend relative to $f_{0.075}$.

4.5. Half-life time of foams produced with multiple solid fractions

A linear correlation has been observed between the half-life time and the percentage of the $f_{0.075}$ fraction relative to the total solid fraction m_x, as depicted in Fig. 26.

Lastly, Fig. 27 illustrates the relationship between foamability and half-life for all tests conducted with varying proportions of $f_{0.075}$ and $f_{0.125}$, merging the results of Fig. 25 and Fig. 26. This analysis also

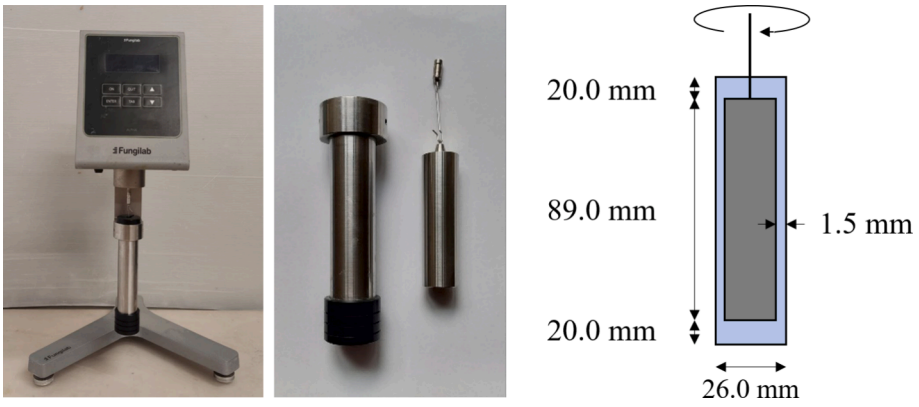

Fig. 12. Rotational viscometer and LCP spindle.

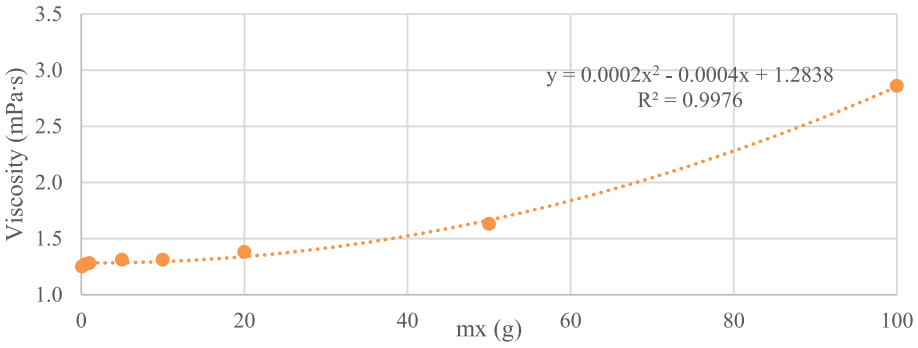

Fig. 13. Viscosity vs solid fraction for $f_{0.075}$.

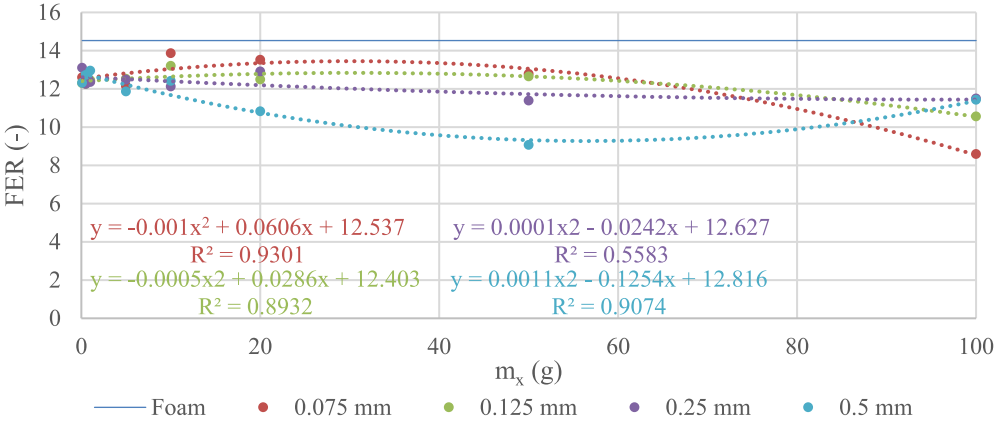

Fig. 14. Foamability vs m_x for different f_x. Average data (five values for each data point) are plotted.

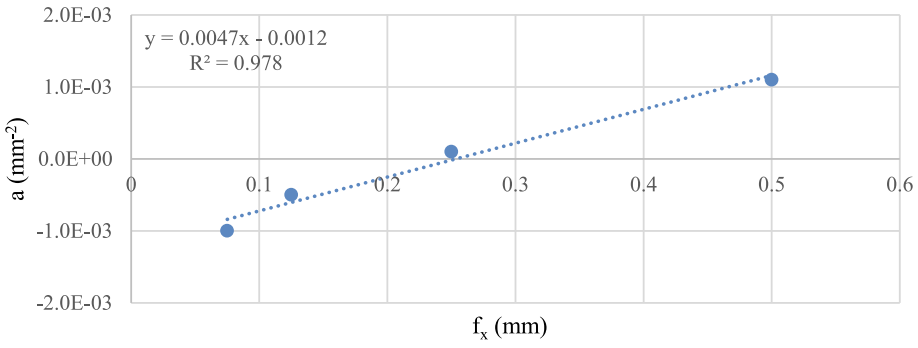

Fig. 15. Second degree coefficient of interpolation vs particle diameter.

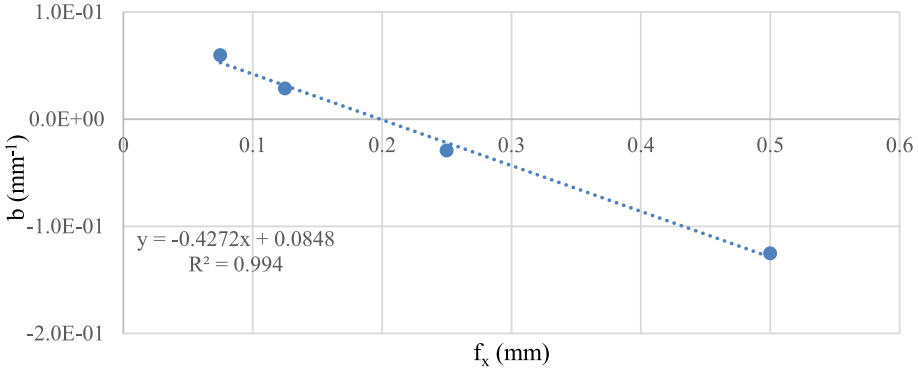

Fig. 16. First degree coefficient of interpolation vs particle diameter.

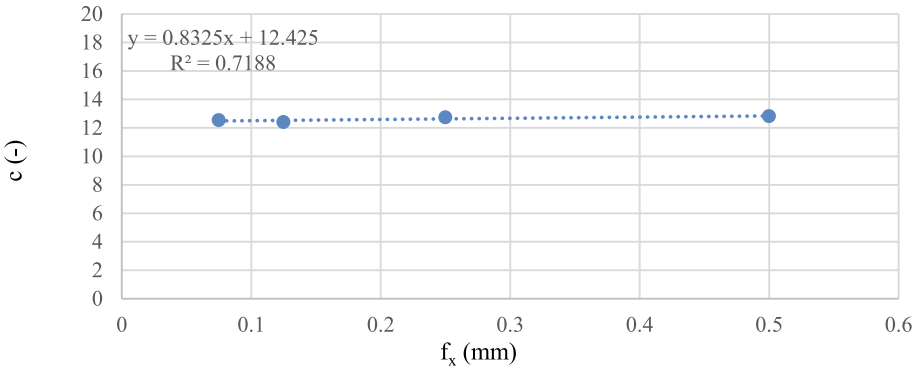

Fig. 17. Zero-degree coefficient of interpolation vs particle diameter.

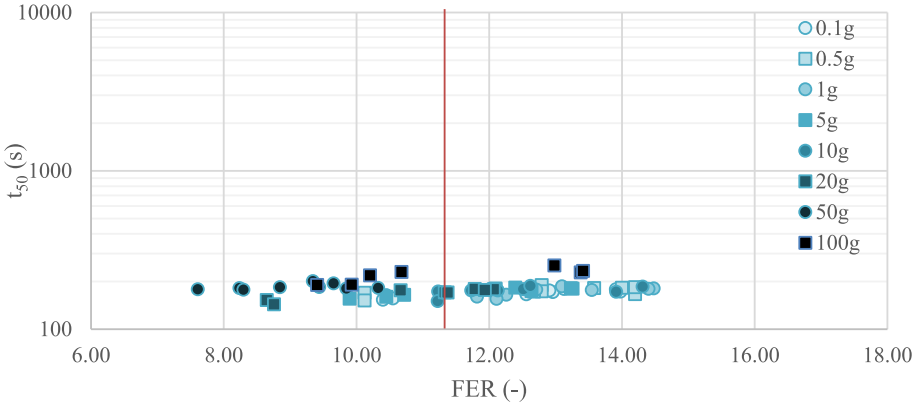

Fig. 18. Half-life vs FER for all m_x and $f_{0.500}$.

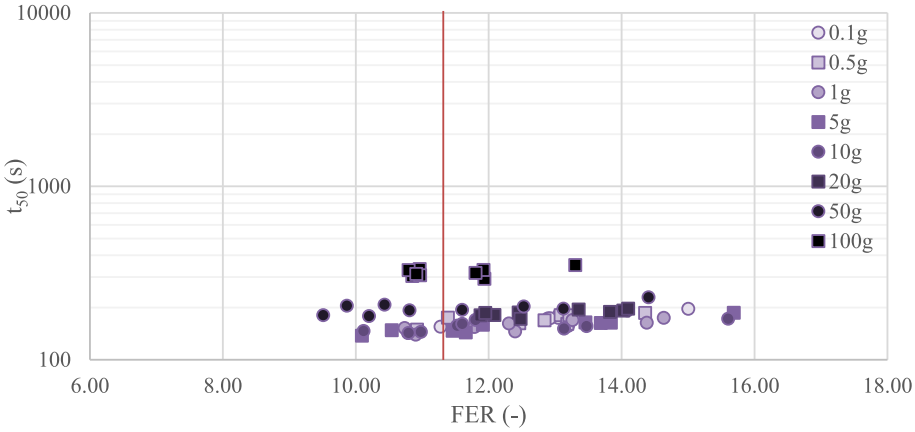

Fig. 19. Half-life vs FER for all m_x and $f_{0.250}$.

revealed a linear trend (Fig. 27), allowing the definition of a linear relationship connecting the three variables: half-life, foamability, and fraction proportions.

4.6. Relationship of half-life time and total surface of the solid fraction

All the conducted tests were further analysed by examining the relationship between the total surface area of the aggregates in the mix and the foam stability. The total surface area of the aggregates was calculated using the following equation, assuming, for simplicity, spherical particles:

$$S = n \bullet s = n \bullet 4\pi(d/2)^2 = n\pi d^2 \tag{3.1}$$

where S represents the total surface area, n is the number of solid particles, s is the surface area of a single particle, and d is the particle diameter. For simplicity, the sieve diameter at which the particles pass was used instead of the actual particle diameter. The number of particles, n, is defined as:

$$n = \frac{V}{v} = \frac{\frac{m}{\gamma_s}}{\frac{4}{3}\pi\left(\frac{d}{2}\right)^3} = \frac{m}{\gamma_s} \bullet \frac{6}{\pi d^3} \tag{3.2}$$

where V is the total volume of the solid particles in the mix, v is the volume of a single particle, γ_s is the specific weight of the solid, and m is the mass of the solid fraction.

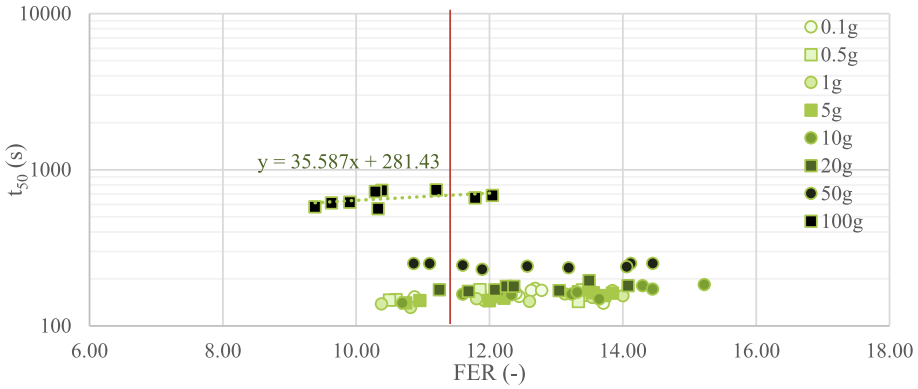

Fig. 20. Half-life vs FER for all m_x and $f_{0.125}$.

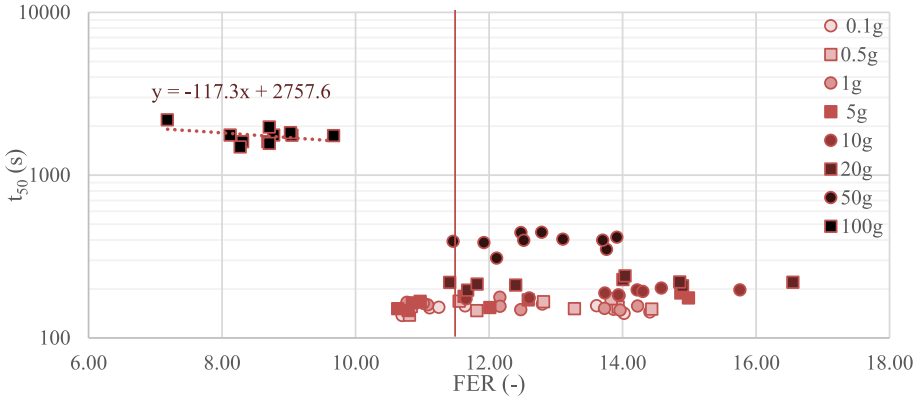

Fig. 21. Half-life vs FER for all m_x and $f_{0.075}$.

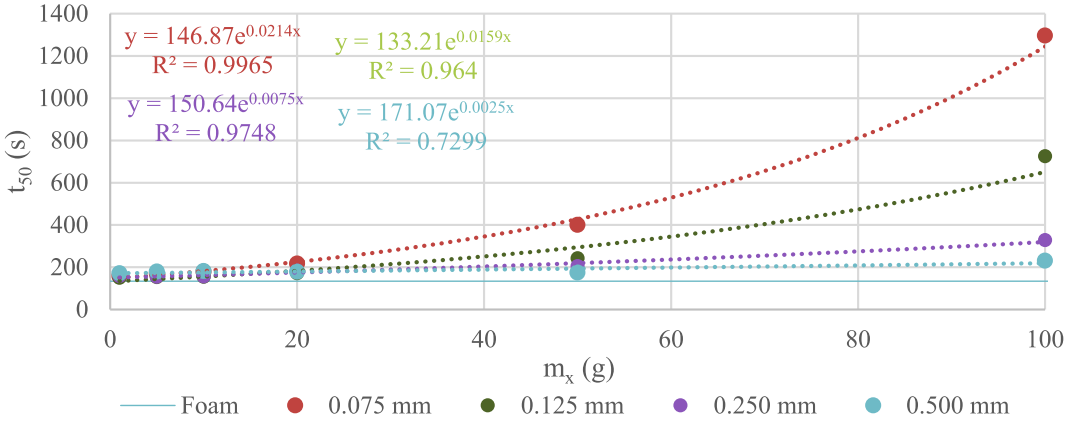

Fig. 22. Half-life time vs m_x for the different f_x. The half-life time of foam without solid particles is plotted as comparison. The values are obtained through interpolation in order to be at constant FER.

Substituting n into Equation (3.1) yields:

$$S = \frac{m}{\gamma_s} \bullet \frac{6}{\pi d^3} \bullet \pi d^2 = \frac{6m}{d\gamma_s} \tag{3.3}$$

Using Equation (3.3), a relationship was found between the total surface area of the solid fraction and the half-life of the foam-aggregate mix, as shown in Fig. 28.

5. Discussion

The tests revealed that foams produced by incorporating soil particles, with varying granulometric fractions (f_x) and solid fractions (m_x), exhibited differences in foamability and stability. Figs. 14 through 21 illustrate the influence of soil particles on the foamability of the foaming solution. This relationship follows a quadratic law and a trend of its polynomial coefficients relative to particle diameter was found.

For small particles, foamability initially increases with an increase in the solid fraction (m_x), reaches a peak and then declines. Conversely, for larger particles, the trend is reversed: foamability initially decreases and then rises as m_x increases beyond a certain value. Although the exact mechanisms driving this behaviour remain unclear, a theoretical model is proposed to explain these observations.

The foaming process is strongly influenced by surfactant concentration. As m_x increases, more surfactant is adsorbed onto the solid

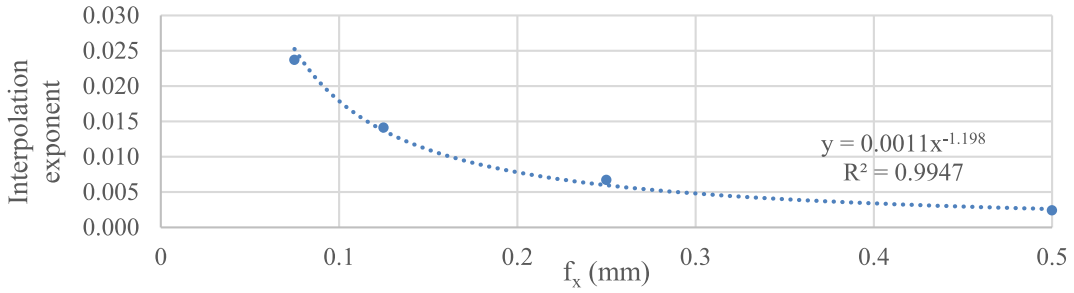

Fig. 23. The exponents of the trend lines of Fig. 22 as function of fractions' particle diameter.

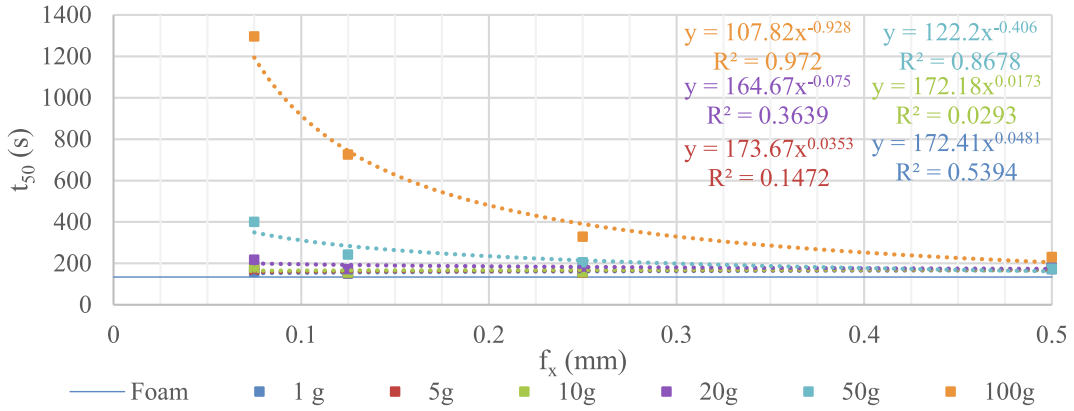

Fig. 24. Half-life time vs f_x for different m_x. $m_{0.1}$ and $m_{0.5}$ are not plotted since not significatively different from $m_{1.0}$.

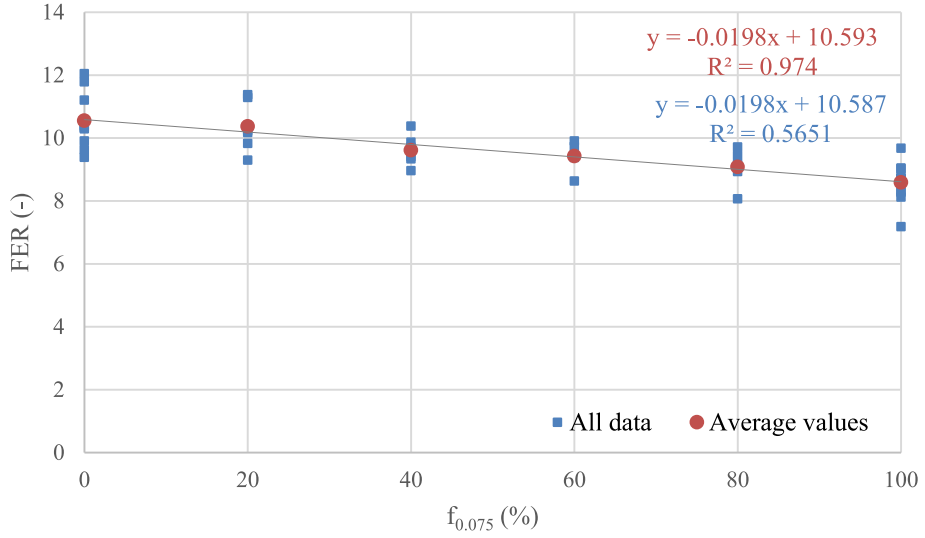

Fig. 25. FER as function of the percentage of $f_{0.075}$ in the total solids for m_{100}.

surface (Phenomenon 1), reducing the available surfactant concentration and, consequently, foamability. Additionally, smaller particles reduce surface tension, as demonstrated by AlYousef (2018) (Phenomenon 2), counteracting the effect of surfactant adsorption. Moreover, fine particles increase the viscosity of the liquid phase, lowering the efficiency of air incorporation into the foam (Phenomenon 3). Lastly, as particle diameter increases, it is hypothesized that their influence on turbulence enhances the dispersion of air within the medium (Phenomenon 4), as illustrated in Fig. 29.

The interaction of these four phenomena varies in intensity as m_x and f_x change, as qualitatively illustrated in Fig. 30.

The results obtained at the target FER revealed the influence of particle diameter and solid fraction on foam half-life time. Specifically, as the solid fraction (m_x) increases, the half-life time of the foam rises exponentially. Conversely, as the diameter of the solid particles increases, the half-life time decreases, following a power law. The effects of the solid fraction became significant for m_x values exceeding 50 g and particle diameters smaller than 0.125 mm.

Additionally, an exponential relationship was observed between the half-life time of foam-aggregate mixtures and the total surface area of the aggregates in the mixture. For tests involving two fractions combined in varying proportions, it was found that their contributions to both time stability and foamability are linearly dependent on the quantity of each fraction.

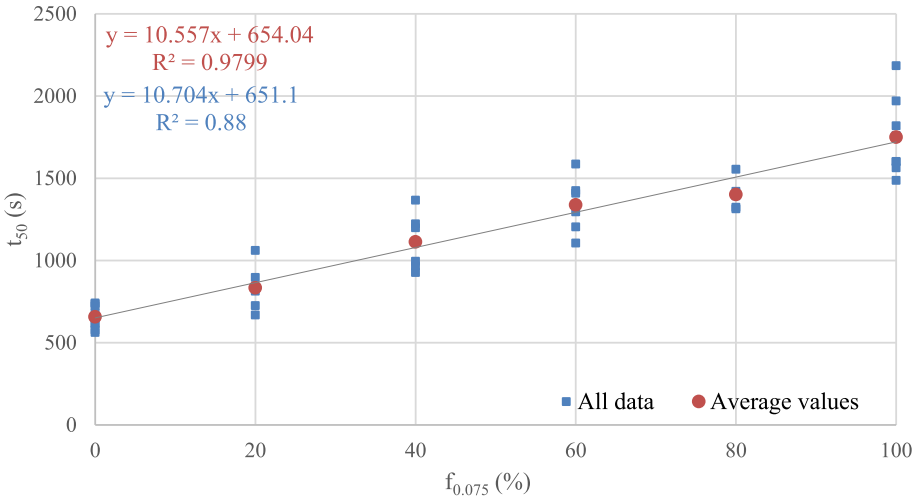

Fig. 26. Half-life time as function of the percentage of $f_{0.075}$ in the total solids for m_{100}.

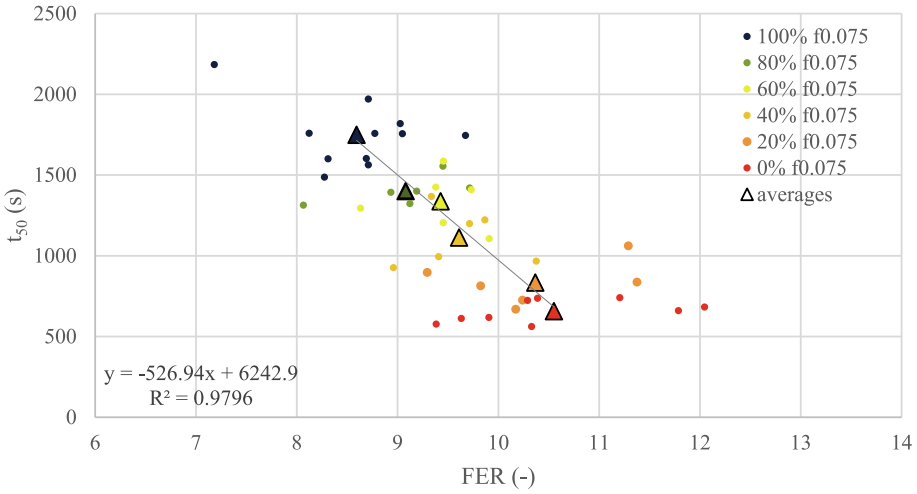

Fig. 27. Half-life time vs foamability for all the mix.

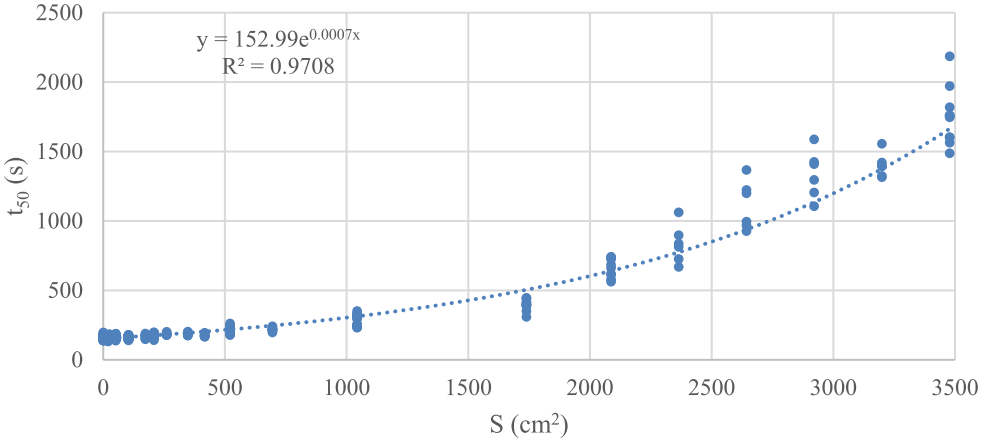

Fig. 28. Particles' total surface area vs half-life time. All the tests with all the types and quantities of solids particles are plotted.

It is also important to acknowledge that in actual EPB-TBM operations, the mixing of foam and soil occurs within the excavation chamber under pressurized conditions. While the present study was conducted at atmospheric pressure, the effect of higher pressure on foam stability is generally positive. According to Boyle's law, increased pressure leads to a reduction in bubble size. Smaller bubbles usually exhibit higher stability due to reduced drainage rates and increased resistance to coalescence (Wu et al., 2018). Consequently, the stability results obtained in this study at atmospheric pressure can be considered a conservative estimate (or a lower bound) of the actual performance in the excavation

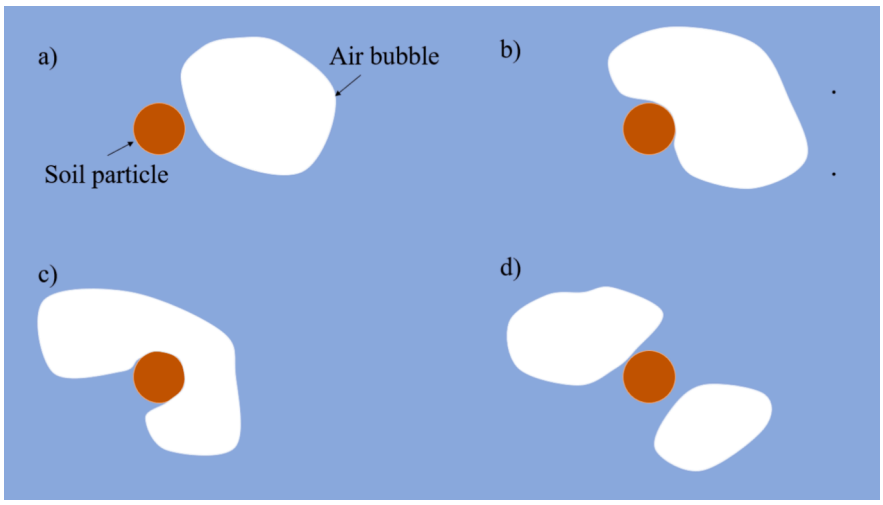

Fig. 29. Phenomenon 4: During the mixing, the solid particles collide with air bubbles and contribute to separate them in smaller and more stable bubbles.

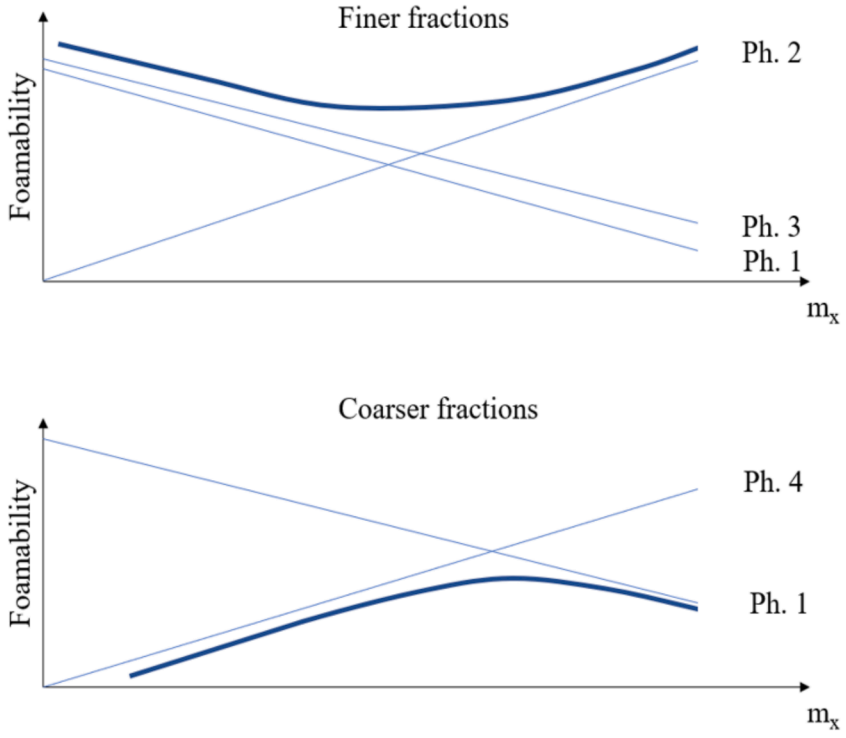

Fig. 30. Qualitative representation of the interplay of different phenomena (Ph.) on foamability.

chamber. Although the absolute values of half-life time might increase under pressure, the observed trends regarding the interaction between particle size (f_x), solid fraction (m_x), and foam stability are expected to remain valid and representative of the relative influence of soil properties on conditioning.

Considering the average FER used in the tests (12.46), the amount and density of the foaming solution ($w_{lg} = 125$ g and $\gamma_{lg} = 1$ g/cm^3, respectively), a solid fraction (m_x) ranging from 0.1 g to 100 g, and using a soil bulk density (γ_b) of 18 kN/m^3 as a reference, the FIR was calculated as:

$$FIR(\%) = \frac{\frac{w_{lg}}{\gamma_{lg}} FER}{\frac{m_x}{\gamma_b}} \bullet 100 \quad (3.4)$$

This yields to FIR values ranging from $3{\cdot}10^3$%·to $3{\cdot}10^6$%, as schematically shown in Fig. 31. Hence, the tests were conducted with a FIR that was two orders of magnitude higher than the typical values used in soil conditioning and the tests were performed at atmospheric pressure. Due to this gap, the validity of these findings is constrained to this FIR range and higher FIR values, for which no distinction exists between the foam-aggregate mixture and pure foam. On the other hand, for FIR values below the lower limit, it is unlikely that the exponential increase in stability continues, as drainage would become so minimal that evaporative effects could no longer be neglected.

6. Conclusions

This study investigated the stability of foam-soil mixtures to bridge the gap between pure foam analysis and conditioned soil behaviour in EPB tunnelling. The experimental results confirm that the inclusion of

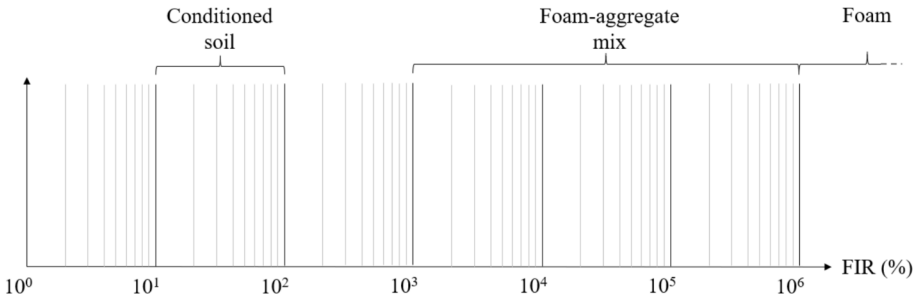

Fig. 31. FIR ranges for conditioned soil, foam-aggregate mix and foam.

particles in foam significantly enhances its stability. Specifically, stability was found to increase exponentially with the solid fraction (m_x) and decreases according to a power law as the particle diameter increases. The stabilizing effect becomes particularly pronounced for solid fractions exceeding 50 g (per 125 g of foaming solution) and for particle diameters smaller than 0.25 mm.

A key finding of this research is that the contributions of different granulometric fractions to stability are additive. Consequently, the stability of foam-solid mixtures can be expressed as an exponential function of the total surface area of the particles. This correlation underscores the dominant role of finer particles in extending foam half-life.

Furthermore, the study highlights the complex influence of solid particles on foamability. The results suggest a dual mechanism involving alterations in surface tension and liquid phase viscosity. While previous literature hinted at these effects for fine particles, this research expands the understanding to include the behaviour of larger particles diameters, which were previously underexplored.

Although a discrepancy remains between the Foam Injection Ratios (FIR) achieved in this laboratory setup and those typical of on-site soil conditioning, this work successfully narrows the experimental gap. By quantifying the stabilizing role of specific solid fractions, this study provides a robust foundation for future research aimed at fully predicting the time-stability of conditioned soil in EPB applications for different types of soils.

CRediT authorship contribution statement

Andrea Carigi: Writing – review & editing, Writing – original draft, Visualization, Methodology, Investigation, Formal analysis, Data curation, Conceptualization. **Carmine Todaro:** Writing – review & editing, Supervision.

Declaration of competing interest

The authors declare that they have no known competing financial interests or personal relationships that could have appeared to influence the work reported in this paper.

Data availability

Data will be made available on request.

References

AlYousef, Z.A., Almobarky, M.A., Schechter, D.S., 2018. The effect of nanoparticle aggregation on surfactant foam stability. J. Colloid Interface Sci. 511, 365–373.
Bahrami, N., Carigi, A., Todaro, C., 2024. Evaluation of the time-dependency of mechanical parameters of conditioned cohesionless soils. Tunn. Undergr. Space Technol. 150, 105828.
Budach, C., & Thewes, M. (2015). Application ranges of EPB shields in coarse ground based on laboratory research. Tunnelling and Underground Space Technology Incorporating Trenchless Technology Research, 50, 296–304. https://doi.org/10.1016/j.tust.2015.08.006.
Carigi, A., Todaro, C., Martinelli, D., Amoroso, C., & Peila, D. (2020). Evaluation of the Geo-Mechanical Properties Property Recovery in Time of Conditioned Soil for EPB-TBM Tunneling, 10(11), 438, https://doi.org/10.3390/geosciences10110438.
Carigi, A., Todaro, C., Martinelli, D., Peila, D., 2022. A more comprehensive way to analyse foam stability for EPB tunnelling – introduction of a mathematical characterization. Geosciences 12 (5), 191.
Carigi, A., Saltarin, S., Di Giovanni, A., Todaro, C., Peila, D., 2023. Reuse of EPB mucking for concrete production: a laboratory test campaign. Case Stud. Constr. Mater. 18, e02187. https://doi.org/10.1016/j.cscm.2023.e02187.
Chen, Z., Bezuijen, A., Fang, Y., Thewes, M., Zheng, D., 2024. The study of foaming agent concentration choice in EPB shield conditioning. Acta Geotech. 1–16. https://doi.org/10.1007/s11440-024-02445-2.
Djeran-Maigre, I., Dubujet, P., Vogel, T.M., 2018. Variation over time of excavated soil properties treated with surfactants. Environ. Earth Sci. 77, 1–12.
EFNARC (2005). Specification and guidelines for the use of specialist products for Mechanized Tunnelling (TBM) in Soft Ground and Hard Rock. Recommendation of European Federation of Producers and Contractors of Specialist Products for Structures.
Fameau, A.L., Salonen, A., 2014. Effect of particles and aggregated structures on the foam stability and aging. C. R. Phys. 15 (8–9), 748–760.
Firouzei, Y., Grenni, P., Barra Caracciolo, A., Patrolecco, L., Todaro, C., Martinelli, D., Carigi, A., Hajipour, G., Hassanpour, J., Peila, D., 2020. The most common laboratory procedures for the evaluation of EPB TBMs excavated material ecotoxicity in Italy: a review. GEAM—Geoingeria Ambientale E Mineraria 160, 44–56.
Grossmann, L., Moll, P., Reichert, C., Weiss, J., 2020. Influence of energy density on foamability: comparison of three foaming methods. Food Res. Int. 129, 108794.
Horozov, T.S., 2008. Foams and foam films stabilised by solid particles. Curr. Opin. Colloid Interface Sci. 13 (3), 134–140.
Hunter, T.N., Wanless, E.J., Jameson, G.J., Pugh, R.J., 2009. Non-ionic surfactant interactions with hydrophobic nanoparticles: impact on foam stability. Colloids Surf A Physicochem Eng Asp 347 (1–3), 81–89.
Jones, S.A., Laskaris, G., Vincent-Bonnieu, S., Farajzadeh, R., Rossen, W.R., 2016. Effect of surfactant concentration on foam: from coreflood experiments to implicit-texture foam-model parameters. J. Ind. Eng. Chem. 37, 268–276.
Li, X., Pu, C., Chen, X., 2022. Improved foam stability through the combination of silica nanoparticle and thixotropic polymer: an experimental study. J. Mol. Liq. 346, 117153.
Luo, G., Xiao, C., Liu, Y., Feng, K., Ren, Q., 2022. Research on the reuse of discharged soil from EBP shield tunnels in synchronous grouting material. Adv. Civ. Eng., 8102488 https://doi.org/10.1155/2022/8102488.
Moll, P., Grossmann, L., Kutzli, I., Weiss, J., 2020. Influence of energy density and viscosity on foam stability – a study with pea protein (Pisum Sativum L.). J. Dispers. Sci. Technol. 41 (12), 1789–1792.
Mori, L., Mooney, M., Cha, M., 2018. Characterizing the influence of stress on foam conditioned sand for EPB tunneling. Tunn. Undergr. Space Technol. 71, 454–465. https://doi.org/10.1016/j.tust.2017.09.018.
Oggeri, C., Fenoglio, T.M., Vinai, R., 2014. Tunnel spoil classification and applicability of lime addition in weak formations for muck reuse. Tunn. Undergr. Space Technol. 44, 97–107.
Oñate, C., & T. Murt. (2022). Environmentally Friendly Soil Conditioning for EPB TBM: The State of Environmental Considerations in North America and Around the World. North American Tunneling 2022 Proceedings.
Pedraza Peña, A.F., Selmi, M., Zyed, M., Dubujet, P., Kacem, M., Murillo Feo, C.A., 2015. Temporal analysis of side effects produced by foam agents in the soil excavated with Earth Pressure Balance (EPB). Ingeniería Civil.
Peila, D., Oggeri, C., Vinai, R., 2007. Screw conveyor device for laboratory tests on conditioned soil for EPB tunneling operations. J. Geotech. Geoenviron. Eng. 133 (12), 1622–1625.
Peila, D., Oggeri, C., & Borio, L. (2008). Influence of granulometry, time and temperature on soil conditioning for EPBS applications. In Proceedings World Tunnel Congress (Vol. 2008, pp. 22-24).
Peila, D., Picchio, A., Chieregato, A., 2013. Earth pressure balance tunnelling in rock masses: laboratory feasibility study of the conditioning process. Tunn. Undergr. Space Technol. 35, 55–66.
Peila, D., Todaro, C., Carigi, A., Padulosi, S., & Martelli, F. (2022). Environmental aspects. In Handbook on Tunnels and Underground Works: Volume 1: Concept–Basic Principles of Design (pp. 101–118).

Peña Duarte, M. (2007). Foam as a soil conditioner in tunnelling: physical and mechanical properties of conditioned sands (Doctoral dissertation, Oxford University, UK).

Riviera, P.P., Bellopede, R., Marini, P., Bassani, M., 2014. Performance-based re-use of tunnel muck as granular material for subgrade and sub-base formation in road construction. Tunn. Undergr. Space Technol. 40, 160–173.

Schröer, M., Gramlich, N., Thewes, M., Langmaack, L., 2023. Expanding the application range of EPB shields using SolidFoam. In: Expanding Underground-Knowledge and Passion to Make a Positive Impact on the World. CRC Press, pp. 1437–1444.

Todaro, C., Peila, L., Luciani, A., Carigi, A., Martinelli, D., Boscaro, A., 2019. Two component backfilling in shield tunneling: Laboratory procedure and results of a test campaign. In: Tunnels and Underground Cities: Engineering and Innovation Meet Archaeology, Architecture and Art- Proceedings of the WTC 2019 ITA-AITES World Tunnel Congress, pp. 3210–3223. https://doi.org/10.1201/9780429424441-340.

UNI EN 933-1 Tests for geometrical properties of aggregates, determination of particle size distribution, sieving method.

UNI EN ISO 17892-12:2018 Geotechnical investigation and testing – Laboratory testing of soil – Part 12: Determination of liquid and plastic limits.

Vinai, R., Oggeri, C., Peila, D., 2008. Soil conditioning of sand for EPB applications: a laboratory research. Tunn. Undergr. Space Technol. 23, 308–317.

Wierenga, P.A., van Norél, L., Basheva, E.S., 2009. Reconsidering the importance of interfacial properties in foam stability. Colloids Surf. A. Physiochem. Eng. Asp. 344, 72–78.

Wu, Y., Mooney, M.A., Cha, M., 2018. An experimental examination of foam stability under pressure for EPB TBM tunneling. Tunn. Undergr. Space Technol. 77, 80–93.

Wu, Y., Nazem, A., Meng, F., Mooney, M.A., 2020. Experimental study on the stability of foam-conditioned sand under pressure in the EPBM chamber. Tunn. Undergr. Space Technol. 106, 103590.

Wu, T., Gao, Y., Huang, C., Jin, A., Qu, X., Ji, M., Zhou, Y., Li, J., 2024. In situ resource reutilization of earth pressure balance (EPB) shield muck for the generation of novel synchronous grouting materials. Constr. Build. Mater. 421, 135737. https://doi.org/10.1016/j.conbuildmat.2024.135737.

Zhang, Y., Chang, Z., Luo, W., Gu, S., Li, W., An, J., 2015. Effect of starch particles on foam stability and dilatational viscoelasticity of aqueous-foam. Chin. J. Chem. Eng. 23, 276–280.

Zhao, S., Li, S., Wan, Z., Wang, X., Wang, M., Yuan, C., 2021. Effects of anticlay agents on bubble size distribution and stability of aqueous foam under pressure for earth pressure balance shield tunneling. Colloid and Interface Science Comminication 42, 100424.

Zumsteg, R., Plotze, M., Puzrin, M., 2018. Leaching characteristics of chemicals from conditioned tunnelling muck. J. Geotech. Geoenviron. Eng. 144 (2).